# Supramolecular organization of the organic-inorganic hybrid $[\{p\text{-}(CH_3)_2NH—C_6H_4—NH_3\}_2Cl][BiI_6]$: assembly of a three-dimensional structure *via* covalent and non-covalent interactions

*T. A. Shestimerova,[a] N.A. Golubev,[a] A. V. Grigorieva,[a,b] M. A. Bykov,[a] Z. Wei,[c] E. V. Dikarev,[c] and A. V. Shevelkov[a]★*

[a]*Department of Chemistry, Lomonosov Moscow State University, Build. 3, 1 Leninskie Gory, 119991 Moscow, Russian Federation. E-mail: shev@inorg.chem.msu.ru*
[b]*Department of Materials Science, Lomonosov Moscow State University, Build. 73, 1 Leninskie Gory, 119991 Moscow, Russian Federation*
[c]*Department of Chemistry, University at Albany, Albany, New York 12222, United States*

A new organic-inorganic hybrid $[\{p\text{-}(CH_3)_2NH—C_6H_4—NH_3\}_2Cl][BiI_6]$ was synthesized and its crystal structure was established. The hybrid consists of an inorganic anion $[BiI_6]^{3-}$ and an organic cation $[\{p\text{-}(CH_3)_2NH\text{-}C_6H_4\text{-}NH_3\}_2Cl]^{3+}$. The $[BiI_6]^{3-}$ anions are linked *via* non-covalent I···I interactions between axial atoms of neighboring anions to form chains running along the *c* axis of the tetragonal unit cell. In the cationic part, the $Cl^-$ anion is involved in four (N)H···Cl hydrogen bonds with hydrogen atoms of the $p\text{-}(CH_3)_2NH—C_6H_4—NH_3^{2+}$ cation, forming a two-dimensional substructure. Alternating covalent and I···I halogen bonds in the anionic substructure and cation—anion hydrogen bonds provide the formation of a three-dimensional supramolecular structure with a band gap of 1.93 eV.

**Key words:** supramolecular structure, organic-inorganic hybrid, halobismuthates, crystal structure, Raman spectroscopy.

The chemistry of halometallates of main-group metals has attracted growing interest in recent years. The discovery of perovskite-like iodoplumbates with remarkable photovoltaic properties[1,2] has stimulated the development of the chemistry of other elements capable of forming such compounds as potential dyes for photovoltaics to achieve efficient conversion of visible light of the solar spectrum into electrical current.[3—5] Such elements include, in particular, bismuth, which is the closest neighbor of lead in the Periodic table and the heaviest non-radioactive element.

Currently, the efficiency of solar cells based on halobismuthates is at most 3% (see Refs 6—8), which is seven times lower than the efficiency of perovskite-like haloplumbates.[1] Nevertheless, according to modern concepts, bismuth in oxidation state +3 has properties required for its compounds to be potential light-absorbing materials for solar cells.[9,10] The $Bi^{3+}$ cation has a highly polarizable electron cloud with an inert $6s^2$ lone pair, showing no pronounced stereo activity. The Bi atom is characterized by strong spin-orbit coupling. Besides, in oxidation state +3, bismuth does not undergo redox reactions. Finally, which is very important, bismuth, unlike lead, has no significant toxicity. However, the lack of knowledge about all the factors, which are responsible for photovoltaic activity of halometallates, makes it impossible to reliably predict the structure—property relationship for these compounds. Hence, the control of the band gap is the only efficient approach to creating halobismuthate-derived light-absorbing materials.

Most of iodometallates containing isolated $[BiI_6]^{3-}$ anions exhibit a wide band gap of 2.15—2.30 eV,[9,10] with rare exceptions.[11] Currently, there are several methods of controlling the band gap. Apart from the efficient approach based on the design of polymeric structures,[7,12—17] the formation of systems of non-covalent bonds has been applied for this purpose in the past 3—4 years. There are four lines of research on the utilization of non-covalent bonds to decrease the band gap of halometallates. First, it was shown that the band gap is affected by hydrogen bonds, in particular (N)H···I bonds with a length from 2.5 to 2.8 Å between iodine atoms of $[BiI_6]^{3-}$ anions and protons of nitrogen-containing organic cations.[18] Second, so-called secondary I···I interactions (3.3—3.5 Å) between iodine atoms of $[BiI_6]^{3-}$ anions and additional $I_2$ molecules or $I_3^-$ anions in the crystal structure play a significant role.[19—22] Besides, it was found that even long-range I···I

Published in Russian in *Izvestiya Akademii Nauk. Seriya Khimicheskaya,* No. 1, pp. 39—46, January, 2021.

interactions between adjacent $[BiI_6]^{3-}$ anions with a length of 3.8—3.9 Å can provide the narrowing of the band gap of iodometallates.[23,24] Finally, several compounds, in which halogen bonds are formed between cations and anions, were descrribed;[25—27] however, the synthesis of such compounds has not yet been reported for iodobismuthates.

Here, we report the synthesis and characterization of new hybrid iodobismuthate $[\{p\text{-}(CH_3)_2NH—C_6H_4—NH_3\}_2Cl][BiI_6]$ (**1**). The crystal structure of **1** can be described as a combination of a two-dimensional organic cation and a one-dimensional inorganic anion. An alternation of covalent, hydrogen, and halogen bonds in the cationic and anionic substructures and cation—anion hydrogen bonds results in the formation of a three-dimensional covalent structure with a band gap of 1.93 eV.

## Experimental

Bismuth (granular, 99.99%), $I_2$ (analytical grade), red phosphorus ($P_{red}$, high-purity grade), 4-(*N*,*N*-dimethyl)phenylenediammonium dichloride (analytical grade), and ethanol (high-purity grade) were used as the starting compounds. Bismuth triiodide $BiI_3$ was prepared by the ampoule method; acid HI (stabilized) was produced by the hydrolysis of freshly prepared $PI_3$ followed by the distillation. The corresponding procedures were described in detail in the study.[12]

**Synthesis of compound 1.** A mixture (0.88 g) of 4-(*N*,*N*-dimethyl)phenylenediammonium dichloride and bismuth triiodide in a ratio of 1 : 1 and 1 : 2 for **1a** and **1b**, respectively, was dissolved in a mixture of ethanol (50 mL) and 50% HI (1 mL). The red crystals that formed within a few hours were filtered off and dried in air.

**Powder X-ray diffraction (PXRD) analysis** was performed using a high-resolution Guinier camera (Image Plate Huber G670, Cu-$K_{\alpha 1}$ radiation, λ = 1.54051 Å) at room temperature in the 2θ angle range from 3 to 100° with a step width of 0.005°; the exposure time was 1200 s. Before the PXRD, the crystals were thoroughly ground in an agate mortar, and the resulting powder was placed between two X-ray transparent films.

**Thermogravimetric analysis** was performed on a NETZSCH 449 Jupiter simultaneous thermal analyzer. The measurements were carried out in a dry argon flow in the temperature range of 23—400 °C at a heating rate of 5 °C $min^{-1}$. Dry calcium oxalate was used as the calibration standard.

**Single-crystal X-ray diffraction study of samples 1a and 1b.** Single-crystal X-ray diffraction data for sample **1a** were collected on a Bruker D8 VENTURE diffractometer equipped with a PHOTON 100 CMOS detector at 100 K using MoKα radiation (λ = 0.71073 Å). The X-ray diffraction data were processed with the Bruker SAINT software; the empirical absorption correction was applied with the SADABS program.[28] The structure was solved by direct methods using the SHELXL program package[29] and refined by the full-matrix least-squares method with the OLEX2 software.[30] Iodine and bismuth atoms and the crystallographically independent chlorine atom were found by direct methods. Initial positions of carbon and nitrogen atoms of the organic cation were located in difference Fourier maps after the refinement of anisotropic displacement parameters of the heavy atoms. The refinement led to a sharp decrease in the *R* factor when the I(2) site was described as occupied by both I and Cl (0.59 : 0.41). The further refinement revealed a disorder at the cation site (0.53 : 0.47) and showed that the I(4) site contains about 12% of chlorine atoms. All nonhydrogen atoms were refined

**Table 1.** Crystallographic data and the structure refinement statistics for **1a** and **1b**

| Parameter | **1a** | **1b** |
|---|---|---|
| Composition | $(C_8H_{14}N_2)_4(BiI_{5.88}Cl_{0.12})(BiI_{5.18}Cl_{0.82})Cl_2$ | $(C_8H_{14}N_2)_4(BiI_{5.47}Cl_{0.53})(BiI_{4.52}Cl_{1.48})Cl_2$ |
| Crystal system | Tetragonal | Tetragonal |
| Space group | *P*4/*ncc* (№ 130) | *P*4/*ncc* (№ 130) |
| *a*/Å | 17.7239(6) | 17.7184(4) |
| *c*/Å | 19.1733(10) | 18.9342(9) |
| *V*/Å$^3$ | 6023.0(5) | 5944.2(4) |
| *Z* | 4 | 4 |
| $d_{calc}$/g $cm^{-3}$ | 2.734 | 2.660 |
| Radiation | MoKα | Synchrotron |
| λ | 0.71073 | 0.420 |
| *T*/K | 100(2) | 100(2) |
| Crystal habit | Prism | Prism |
| Crystal size/mm | 0.090×0.050×0.030 | 0.060×0.040×0.03 |
| Absorption correction | Semiempirical | Semiempirical |
| θ-scan range/deg | 2.781—25.471 | 2.787—25.739 |
| Index ranges *h*, *k*, *l* | $-21 \le h \le 21$, $-21 \le k \le 21$, $-23 \le l \le 23$ | $-25 \le h \le 23$, $-25 \le k \le 25$, $-27 \le l \le 27$ |
| $R_{int}$ | 0.0514 | 0.0167 |
| $R/R_w$ [$I > 2\sigma(I)$] | 0.0424/0.0474 | 0.0240/0.0547 |
| GOOF | 1.065 | 1.103 |
| Residual electron density ($\rho_{max}/\rho_{min}$)/e Å$^{-3}$ | 0.778/−0.837 | 2.046/−1.071 |

with anisotropic displacement parameters. The hydrogen atoms at carbon atoms were refined using a rigid body model with $U_{iso}(H) = 1.5U_{eq}(C)$ for methyl groups and $U_{iso}(H) = 1.2U_{eq}(C)$ for the other atoms. The coordinates of all hydrogen atoms bonded to nitrogen atoms were refined independently with $U_{iso}(H) = 1.2U_{eq}(N)$. Two orientations were proposed for the disordered cation in the structure. The geometric parameters of the disordered cations were fixed so that they were identical. The anisotropic displacement parameters of the disordered moieties were treated with a standard uncertainty of 0.004 Å$^2$. Besides, the $U_{ij}$ components were restrained to be equal with a standard uncertainty of 0.01 Å$^2$.

A single crystal selected for **1b** was glued on a glass thread, mounted on a holder, and cooled to 100 K using an Oxford Instruments Cryojet cryosystem. The X-ray diffraction data were collected on a Bruker D8 diffractometer equipped with a Pilatus 3×2M detector modified to use synchrotron radiation at the Chem-MatCARS 15-ID-B beamline at the Advanced Photon Source (Argonne National Laboratory) at 30 keV (λ = 0.41328 Å) with an exposure time per frame of 0.5 s in the φ-scan mode. The beam intensity was manually reduced to avoid overexposure of individual pixels. The X-ray diffraction data were processed using the Bruker APEX3 software package;[29] the empirical absorption correction was applied with the SADABS program.[30] The crystal structure solution and refinement were performed as described for sample **1a**.

The X-ray diffraction data collection and structure refinement statistics for samples **1a** and **1b** are summarized in Table 1. Selected interatomic distances are listed in Tables 2 and 3. Selected hydrogen bond parameters are given in Table 4. The structure refinement statistics, atomic coordinates, all bond lengths, and C—H···I distances can be obtained from the Cambridge Crystallographic Data Centre (CCDC 2000918 and 2001012).

**Spectral studies.** Crystals for the measurement of Raman spectra were selected from the synthesis products. The Raman spectra were recorded on a Renishaw In Via Raman spectrometer in air at room temperature in a backscattering mode for several crystals. A laser with a wavelength λ = 633 nm (Ar, 50 mV) and a Leica DMLM confocal microscope (100′ lens) were used. The focus distance was 250 mm; the laser beam width was 20 μm. A CCD camera (1024×368 pixels) was employed as the detector. Single-crystal silicon (521.5 cm$^{-1}$) was used as a standard for calibration. The data were processed with the WiRE 3.4 software package.

The UV-Vis absorption spectrum was recorded on a Lambda 950 spectrometer (Perkin-Elmer) equipped with a diffuse reflectance attachment in the spectral range of 250—1200 nm at a scan rate of 2 nm s$^{-1}$ using thoroughly ground polycrystalline samples. The absorption data were converted into transmission spectra and analyzed by the Kubelka—Munk method using a model of an indirect band gap semiconductor.[33]

**Table 2**. Selected interamtomic distances (*d*) in the crystal structures of **1a** and **1b**

| Distance | Occupancy Cl (%), **1a**/**1b** | *d*/Å | |
|---|---|---|---|
| | | **1a** | **1b** |
| Bi(1)—I(1) | | 3.0501(5)×4 | 3.0465(2)×4 |
| Bi(1)—I(2)/Cl(2) | 40.8(4)/ 74.0(1) | 2.9593(10)×2 | 2.8798(8)×2 |
| Bi(2)—I(5) | | 2.9765(15) | 2.9834(6) |
| Bi(2)—I(3)/Cl(3) | 11.8(6)/ 53.1(4) | 3.0105(17) | 2.9361(9 |
| Bi(2)—I(4) | | 3.1159(6)×4 | 3.1205(3)×4 |
| I(2)/Cl(2)—I(2)/Cl(2) | | 3.6682(14) | 3.7073(11) |
| I(5)—I(3)/Cl(3) | | 3.5998(18) | 3.5475(10) |

**Table 3.** Selected bond angles (ω) in the crystal structures of **1a** and **1b**

| Angle | ω/deg | |
|---|---|---|
| | **1a** | **1b** |
| I(1)—Bi(1)—I(1) | 178.85(2)×2 | 176.929(9)×2 |
| | 90×4 | 90×4 |
| I(1)—Bi(1)—I(2) | 89.424(12)×4 | 91.535(4)×4 |
| I(2)—Bi(1)—I(2) | 90.577(12)×4 | 88.465(4)×4 |
| | 180 | 180 |
| I(5)—Bi(2)—I(3) | 180 | 180 |
| I(5)—Bi(2)—I(4) | 92.381(17)×4 | 92.225(6)×4 |
| I(3)—Bi(2)—I(4) | 87.624(16) | 87.775(6) |
| I(4)—Bi(2)—I(4) | 175.24(3)×2 | 175.551(11)×2 |
| | 89.901(1)×4 | 89.914(1)×4 |

**Table 4.** Hydrogen bonds in the crystal structures of **1a** and **1b**

| Fragment D–H···A | *d*(D—H)/Å | | *d*(H···A)/Å | | *d*(D···A)/Å | | D—H···A angle/deg | |
|---|---|---|---|---|---|---|---|---|
| | **1a** | **1b** | **1a** | **1b** | **1a** | **1b** | **1a** | **1b** |
| N(1X)—H(1XA)···Cl(1) | 0.888 | 0.888 | 2.299 | 2.252 | 3.141 | 3.131 | 158.01 | 170.51 |
| N(1X)—H(1XB)···I(2)/Cl(2) | 0.884 | 0.875 | 2.363 | 2.323 | 3.235 | 3.159 | 169.04 | 159.66 |
| N(1X)—H(1XC)···I(4) | 0.882 | 0.881 | 2.931 | 2.874 | 3.637 | 3.651 | 138.28 | 147.85 |
| N(2X)—H(2X)···Cl(1) | 0.881 | 0.878 | 2.204 | 2.194 | 3.060 | 3.066 | 163.71 | 171.81 |
| N(1)—H(1A)···Cl(1) | 0.885 | 0.886 | 2.280 | 2.238 | 3.133 | 3.107 | 161.92 | 167.06 |
| N(1)—H(1B)···I(2) | 0.880 | 0.875 | 2.890 | 2.575 | 3.536 | 3.378 | 131.57 | 152.85 |
| N(1)—H(1C)···I(4) | 0.884 | 0.881 | 2.627 | 2.758 | 3.508 | 3.573 | 174.34 | 154.53 |
| N(2)—H(2)···I(4) | 0.880 | 0.877 | 2.851 | 2.743 | 3.567 | 3.562 | 139.67 | 156.19 |

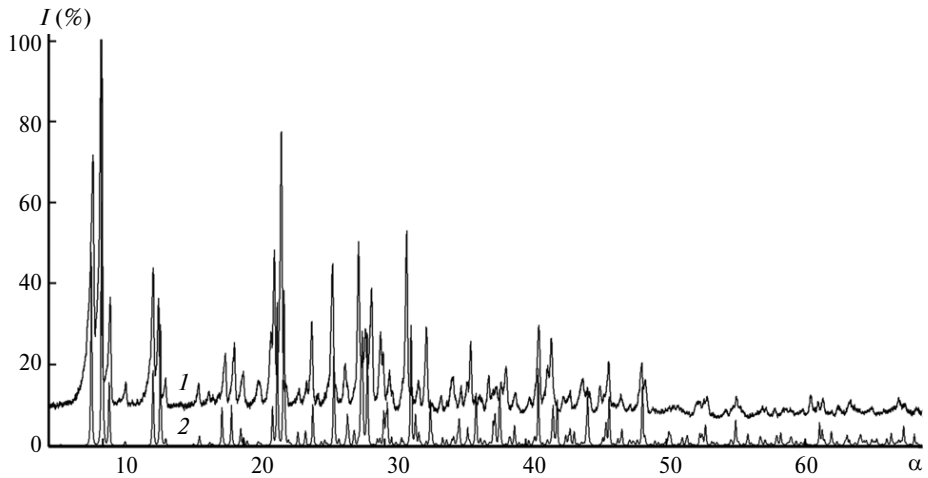


**Fig. 1.** Experimental (*1*) and simulated (*2*) powder X-ray diffraction patterns of compound **1**; α is the Bragg angle.

## Results and Discussion

Red crystals of compound **1** were obtained by the crystallization from an aqueous ethanol solution of hydroiodic acid containing bismuth triiodide and 4-(*N*,*N*-dimethyl)phenylenediammonium dichloride (DMPDA). The reaction products are stable in air. According to the thermogravimetric analysis, the decomposition starts at 150(1) °C. The chlorine content of the crystals varies depending on the concentration of chloride anions in the solution. The experimental X-ray diffraction patterns of two samples are virtually identical to each other and to those simulated based on the single-crystal X-ray diffraction data (Fig. 1).

The crystal structure of **1** is shown in Fig. 2. It consists of two substructures: the cationic organic part of the composition $[\{p\text{-}(CH_3)_2NH—C_6H_4—NH_3\}_2Cl]^{3+}$ and the anionic inorganic part $[BiI_6]^{3-}$.

The anionic inorganic substructure is composed of $[BiI_6]^{3-}$ octahedra, which are linked *via* I···I halogen bonds to form chains running along the *c* axis of the unit cell. There are four chains of octahedra per unit cell. The chains are nonequivalent because two crystallographically independent bismuth atoms, Bi(1) and Bi(2), form their individual chains so that the chains passing through the unit cell represent two equivalent pairs.

In this work, we obtained two types of crystals, which differ in the chlorine content. In these structures, excess

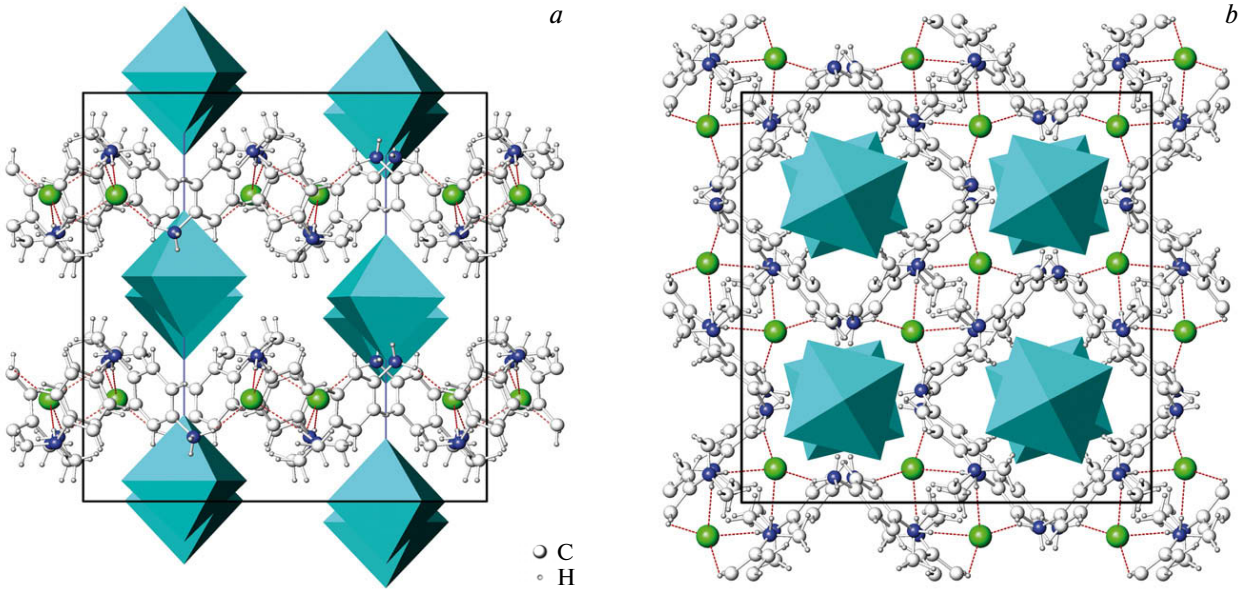


**Fig. 2.** Crystal structure of **1** projected onto the [100] (*a*) and [001] planes (*b*). Chlorine atoms are green, nitrogen atoms are blue, carbon and hydrogen atoms are pale-gray. The $[BiI_6]^{3-}$ octahedra are shown in turquoise, the (N)H···Cl hydrogen bonds are represented by red dashed lines.

chlorine atoms with respect to the ideal composition of compound **1** partially replace iodine atoms at the vertices of $[BiI_6]^{3-}$ octahedra, resulting in the following compositions of the anionic part: $BiI_{5.2}Cl_{0.8}$ (**1a**) and $BiI_{4.5}Cl_{1.5}$ (**1b**) for the Bi(1) octahedra and $BiI_{5.9}Cl_{0.1}$ (**1a**) and $BiI_{5.5}Cl_{0.5}$ (**1b**) for the Bi(2) octahedra. Depending on the chlorine content at the vertices of the octahedra, the Bi—I distances can be different in crystals **1a** and **1b**. Four distances in the equatorial plane of the octahedron, with the I(1) and I(4) sites being occupied exclusively by iodine atoms, are equal in both crystals (Bi(1)—I(1), 3.05 Å; Bi(2)—I(4), 3.12 Å), which is typical of terminal Bi—I bonds in different iodobismuthates.[34] The axial Bi(2)—I(5) distances are also equal (2.98 Å) in both crystals because the I(5) site contains only iodine. On the contrary, other axial distances are significantly different because the I(2) and I(3) sites are partially occupied by chlorine atoms, resulting in the Bi(1)—I(2) distances equal to 2.96 and 2.88 Å in crystals **1a** and **1b**, respectively; the Bi(2)—I(3) distances are 3.01 and 2.94 Å. Despite the presence of chlorine atoms in two sites, the octahedra are only slightly distorted along the fourfold axis; the I—Bi—I bond angles are nearly equal to 90 and 180° (see Table 3).

The $[BiI_6]^{3-}$ octahedra are linked to form chains running along the *c* axis (Fig. 3). However, the strength of halogen—halogen interactions is difficult to evaluate based on the distances between the vertices of adjacent octahedra because the axial I(2) and I(3) sites are occupied together by iodine and chlorine atoms. Nevertheless, we chose the interatomic I(3)···I(5) distance in crystal **1a** for the analysis, because the I(5) site is occupied exclusively by iodine atoms and the percentage of chlorine atoms in the I(3) site is as low as 12%, which cannot exert a significant effect on the interatomic distance equal to 3.60 Å.

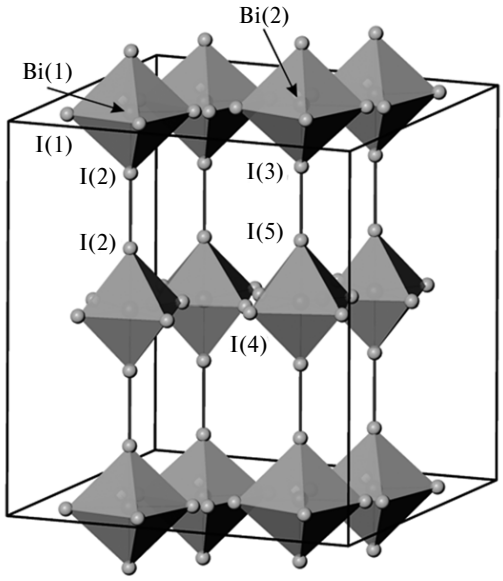


**Fig. 3.** Fragment of chains of $[BiI_6]^{3-}$ octahedra running along the *c* axis in the crystal structure of **1**.

An analysis of the literature data shows that the distances in the range of 3.3—3.5 Å are present in numerous polyiodides containing more than three iodine atoms in the anion (see Refs 35—37). These distances are considered as secondary interactions.[38] Similar distances are observed in polyiodometallates, where the $(M)I\cdots I_2$ distances are at most 3.5 Å.[19,20,39] Only a few triiodides are known, in which the interanionic $I_3\cdots I_3$ distance reaches 3.6 Å.[40] It should be noted that this distance is longer than that of the secondary interaction in crystalline iodine responsible for the semiconducting properties of this simple substance.[41] Meanwhile, the I···I distance in **1a** (3.60 Å) is much shorter than the non-covalent I···I interactions observed between $[BiI_6]^{3-}$ anions in the structures of different iodobismuthates.[20,42,43] Nevertheless, it was noted that even such weak bonds can exert an effect on the band gap, decreasing the latter to 1.9—2.0 eV.[23,43]

The Raman spectrum (Fig. 4) shows that the main vibrations of the anionic substructure appear at low Raman shifts. The peak at 129 $cm^{-1}$ and its visible overtone at 260 $cm^{-1}$ can be assigned to Bi—I stretching vibrations, as described in the literature.[12,44] The shoulder at 100 $cm^{-1}$, marked with an arrow in Fig. 4, corresponds to I···I vibrations, and the peak width is apparently attributed to the joint occupancy of a part of sites by iodine and chlorine atoms, which leads to a certain set of weak I···I and I···Cl bonds with non-equal distances and vibrational energies. Thus, the distances of about 3.3 Å were reported for the I···Cl halogen bond.[45] In the Raman spectra of polyhalides and polyhalometallates, vibrations at 90—105 $cm^{-1}$ are assigned[38] to I···I distances in the range of 3.50—3.60 Å, which correspond to those observed in compound **1** (see Table 2). However, the same spectral region can have both Bi—I bending vibrations and stretching vibrations of the (N)H···I hydrogen bond,[46] and, consequently, the assignment of the broad shoulder at *ca*. 100 $cm^{-1}$ is not unambiguous.

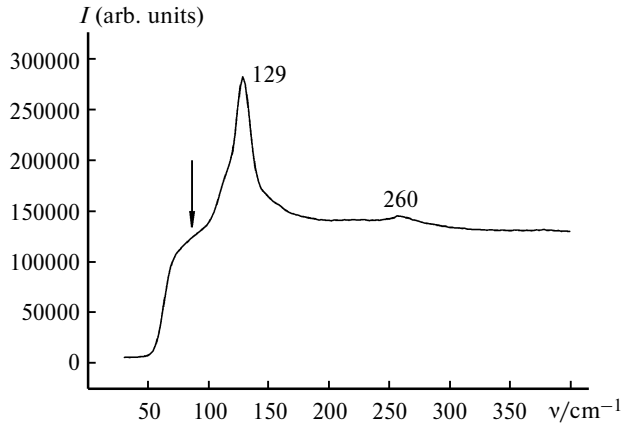


**Fig. 4.** Raman spectrum of compound **1**.

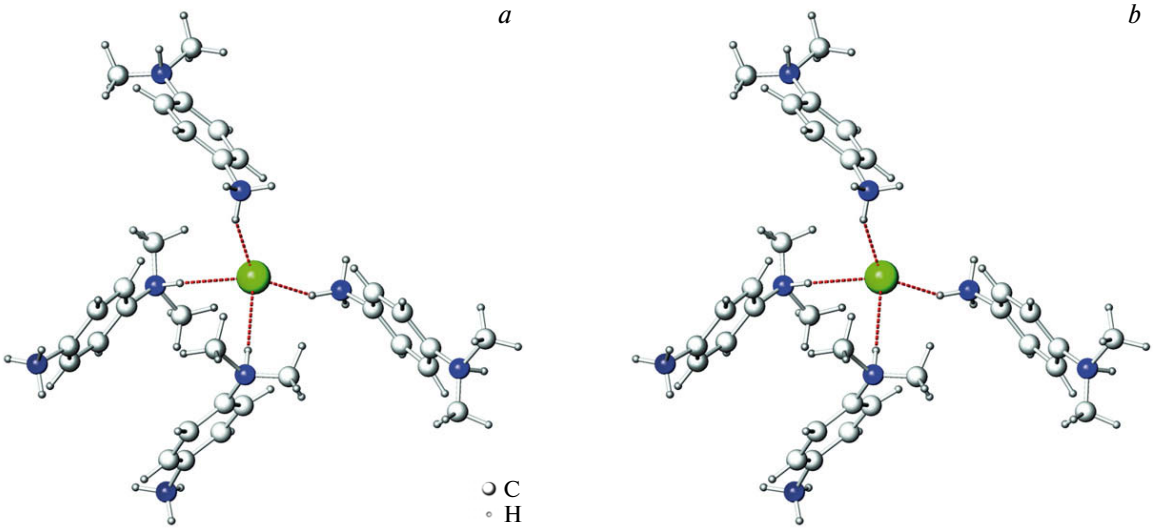


**Fig. 5.** Cationic substructure in the crystal structure of **1**. The environment of $Cl^-$ ions formed by four doubly protonated $[p\text{-}(CH_3)_2NH—C_6H_4—NH_3]^{2+}$ cations (*a*) and a fragment of the cationic layer (*b*). Chlorine atoms are green, nitrogen atoms are blue, carbon and hydrogen atoms are pale-gray, the (N)H···Cl hydrogen bonds are represented by red dashed lines.

The cationic substructure consists of doubly protonated $[p\text{-}(CH_3)_2NH—C_6H_4—NH_3]^{2+}$ cations and $Cl^-$ anions linked together through hydrogen bonds to form a two-dimensional $[\{p\text{-}(CH_3)_2NH—C_6H_4—NH_3\}_2Cl]^{3+}$ network (Fig. 5).

The chlorine atoms are linked by hydrogen bonds to four hydrogen atoms of four different $[p\text{-}(CH_3)_2NH—C_6H_4—NH_3]^{2+}$ cations, resulting in the formation of the distorted tetrahedral environment by hydrogen atoms, with the H—Cl—H angles in the range of 102—127°. In this structure, two $[p\text{-}(CH_3)_2NH—C_6H_4—NH_3]^{2+}$ cations donate $NH_3$ hydrogen atoms and two other cations donate $(CH_3)_2NH$ hydrogen atoms. The local environment of the chlorine atom by hydrogen atoms is described by the crystallographic point group $C_{2v}$. The H···Cl distances are in the range of 2.20—2.30 Å, which is significantly smaller than the typical H···Cl hydrogen bond length (2.5—2.8 Å) and is indicative of its rather high energy.[47]

Interactions between the anionic and cationic substructures in the crystal structure of **1** occur *via* (N)H···I and (C)H···I hydrogen bonds. Since each $[p\text{-}(CH_3)_2NH—C_6H_4—NH_3]^{2+}$ cation contains two $NH_3$ hydrogen atoms, which are not involved in the hydrogen bonding in the cationic substructure, they are accessible for the formation of (N)H···I hydrogen bonds in the cation—anion system. These bond lengths are 2.36 and 2.84 Å. It is worth noting that the latter bond length is typical of (N)H···I hydrogen bonds,[48,49] whereas the former bond length is very rarely observed and is indicative of a high interaction energy.

The (C)H···I hydrogen bonds are much longer, varying in the range from 2.87 to 3.30 Å. The latter distance is only slightly shorter than the sum of the corresponding van der Walls radii, whereas the former distance is comparable with the weakest (N)H···I hydrogen bond. Although the (C)H···I hydrogen bonds are weak, their large number (ten bonds per $[p\text{-}(CH_3)_2NH—C_6H_4—NH_3]^{2+}$ cation) enables strong binding between the anionic and cationic substructures typical of supramolecular assemblies,[50] resulting in the formation of the three-dimensional crystal structure shown in Fig. 2.

The red color of the compound is well consistent with the band gap (1.93 eV) calculated from the diffuse reflectance spectra using the Kubelka—Munk function (Fig. 6). According to the literature data, most of iodobismuthates containing isolated octahedral $[BiI_6]^{3-}$ anions are characterized by a band gap of 2.15—2.30 eV. Exceptions are compounds, in which $[BiI_6]$ octahedra are additionally linked together through hydrogen bonds or secondary

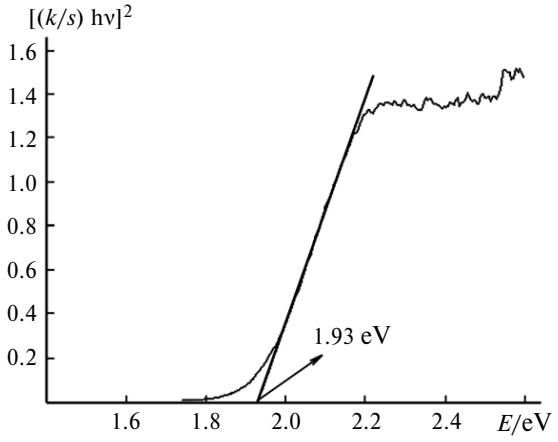


**Fig. 6.** Diffuse reflectance spectrum of compound **1** processed using the Kubelka—Munk model.

interactions, and compounds, in which charge transfer occurs in the cation—anion system.[51] In compound **1**, numerous different types of hydrogen bonds, such as (N)H···Cl, (N)H···I, and (C)H···I, are combined with relatively short secondary I···I interactions, which are responsible for the observed band gap of 1.93 eV.

Therefore, a new organic-inorganic hybrid [{*p*-$(CH_3)_2NH—C_6H_4—NH_3\}_2Cl][BiI_6]$ was synthesized by the reaction of (*p*-$(CH_3)_2NH—C_6H_4—NH_3)Cl_2$ with bismuth triiodide in an aqueous ethanol solution of hydroiodic acid. In the crystal structure of this compounds, the anionic inorganic substructure is composed of $[BiI_6]^{3-}$ octahedra, which are linked by secondary I···I interactions with a length of *ca*. 3.6 Å to form chains running along the *c* axis of the tetragonal unit cell. The two-dimensional cationic organic substructure is formed by the ammonium dication $[p\text{-}(CH_3)_2NH—C_6H_4—NH_3]^{2+}$ and isolated $Cl^-$ anions, which are linked through short H···Cl hydrogen bonds so that each chlorine atom is involved in four hydrogen bonds. The three-dimensional supramolecular structure composed of the cationic and anionic substructures is stabilized by numerous weak (N)H···I and (C)H···I hydrogen bonds. Due to a combination of covalent bonds and numerous non-covalent interactions in the structure of [{*p*-$(CH_3)_2NH—C_6H_4—NH_3\}_2Cl][BiI_6]$, this compound has a band gap of 1.9 eV.

This work was financially supported by the Russian Foundation for Basic Research (Project No. 20-03-00280). Z. Wei and E. V. Dikarev are grateful to the National Science Foundation of USA, the Division of Chemistry (CHE-1955585) and the Division of Materials Research (DMR), for generous financial support of investigations in the ChemMatCARS Sector 15 (Grant NSF/CHE-1834750).

## References

1. W. L. Leong, Z. E. Ooi, D. Sabba, C. Y. Yi, S. M. Zakeeruddin, M. Graetzel, J. M. Gordon, E. A. Katz, N. Mathews, *Adv. Mater.*, 2016, **28**, 2439; DOI 10.1002/adma.201505480.
2. A. Kojima, K. Teshima, Y. Shirai, T. Miyasaka, *J. Am. Chem. Soc.*, 2009, **131**, 6050; DOI 10.1021/ja809598r.
3. A. M. Ganose, C. N. Savory, D. O. Scanlon, *Chem. Commun.*, 2017, **53**, 20; DOI 10.1039/C6CC06475B.
4. Z. Xiao, Z. Song, Y. Yan, *Adv. Mater.*, 2019, **31**, 1803792; DOI 10.1002/adma.201803792.
5. D. H. Fabini, M. Koerner, R. Seshadri, *Chem. Mater.*, 2019, **31**, 1561; DOI 10.1021/acs.chemmater.5b03147.
6. H. Wang, J. Tian, K. Jiang, Y. Zhang, H. Fan, J. Huang, L.-M. Yang, B. Guan, Y. Song, *RSC Adv.*, 2017, **7**, 43826; DOI 10.1039/C7RA07123J.
7. H. C. Sansom, G. F. S. Whitehead, M. S. Dyer, M. Zanella, T. D. Manning, M. J. Pitcher, T. J. Whittles, V. R. Dhanak, J. Alaria, J. B. Claridge, M. J. Rosseinsky, *Chem. Mater.*, 2017, **29**, 1538; DOI 10.1021/acs.chemmater.6b04135.
8. Z. Shao, T. Le Mercier, M. B. Madec, T. Pauporté, *Materials Lett.*, 2018, **221**, 135; DOI: 10.1016/j.matlet.2018.03.085.
9. Y.-Q. Hu, H.-Y. Hui, W.-Q. Lin, H.-Q. Wen, D.-S. Yang, G.-D. Feng, *Inorg. Chem.*, 2019, **58**, 16346; DOI 10.1021/acs.inorgchem.9b01439.
10. G. C. Anyfantis, A. Ioannou, H. Barkaoui, Y. Abid, V. Psycharis, C. P. Raptopoulou, G. A. Mousdis, *Polyhedron*, 2020, **175**, 114180; DOI: 10.1016/j.poly.2019.114180.
11. N. A. Yelovik, T. A. Shestimerova, M. A. Bykov, Z. Wei, E. V. Dikarev, A. V. Shevelkov, *Russ. Chem. Bull.*, 2017, **66**, 1196; DOI: 10.1007/s11172-017-1872-y.
12. N. A. Yelovik, A. V. Mironov, M. A. Bykov, A. N. Kuznetsov, A. V. Grigorieva, Z. Wei, E. V. Dikarev, A. V. Shevelkov, *Inorg. Chem.*, 2016, **55**, 4132; DOI: 10.1021/acs.inorgchem.5b02729.
13. N. Dehnhardt, J.-N. Luy, M. Szabo, M. Wende, R. Tonner, J. Heine, *Chem. Commun.*, 2019, **55**, 14725; DOI: 10.1039/C9CC06625J.
14. Y.-Q. Hu, H.-Y. Hui, W.-Q. Lin, H.-Q. Wen, D.-S. Yang, G.-D. Feng, *Inorg. Chem.*, 2019, **58**, 16346; DOI: 10.1021/acs.inorgchem.9b01439.
15. V. Yu. Kotov, A. B. Ilyukhin, A. A. Korlyukov, A. F. Smol´yakov, S. A. Kozyukhin, *New J. Chem.*, 2018, **42**, 6354; DOI: 10.1039/C7NJ04948J.
16. A. J. Lehner, D. H. Fabini, H. A. Evans, C.-A. Hébert, S. R. Smock, J. Hu, H. Wang, J. W. Zwanziger, M. L. Chabinyc, R. Seshadri, *Chem. Mater.*, 2015, **27**, 7137; DOI: 10.1021/acs.chemmater.5b03147.
17. A. N. Usoltsev, M. Elshobaki, S. A. Adonin, L. A. Frolova, T. Derzhavskaya, P. A. Abramov, D. V. Anokhin, I. V. Korolkov, S. Yu. Luchkin, N. N. Dremova, K. J. Stevenson, M. N. Sokolov, V. P. Fedin, P. A. Troshin, *J. Mater. Chem. A*, 2019, **7**, 5835; DOI: 10.1039/C8TA09204D.
18. T. A. Shestimerova, A. V. Mironov, M. A. Bykov, E. D. Starichenkova, A. N. Kuznetsov, A. V. Grigorieva, A. V. Shevelkov, *Cryst. Growth Design.*, 2020, **20**, 87—94; DOI: 10.1021/acs.cgd.9b00636.
19. T. A. Shestimerova, N. A. Yelavik, A. V. Mironov, A. N. Kuznetsov, M. A. Bykov, A. V. Grigorieva, V. V. Utochnikova, L. S. Lepnev, A. V. Shevelkov, *Inorg. Chem.*, 2018, **57**, 4077; DOI: 10.1021/acs.inorgchem.8b00265.
20. T. A. Shestimerova, N. A. Golubev, N. A. Yelavik, M. A. Bykov, A. V. Grigorieva, Z. Wei, E. V. Dikarev, A. V. Shevelkov, *Cryst. Growth Design*, 2018, **18**, 2572; DOI: 10.1021/acs.cgd.8b00179.
21. W. Zhang, B. Kou, Y. Peng, Z. Wu, Y. Yao, D. Dey, L. Lia, J. Luo, *J. Mater. Chem. C*, 2018, **6**, 12170; DOI: 10.1039/C8TC04372H.
22. S. A. Adonin, A. N. Usoltsev, A. S. Novikov, B. A. Kolesov, V. P. Fedin, M. N. Sokolov, *Inorg. Chem.*, 2020, **59**, 3290; DOI: 10.1021/acs.inorgchem.9b03734.
23. T. Li, Y. Hu, C. A. Morrison, W. Wu, H. Hana, N. Robertson, *Sustainable Energy Fuels.*, 2017, **1**, 308; DOI: 10.1039/C6SE00061D.
24. P. A. Buikin, A. B. Ilyukhin, A. E. Baranchikov, K. E. Yorov, V. Yu. Kotov, *Mendeleev Commun.*, 2018, **28**, 490; DOI: 10.1016/j.mencom.2018.09.012.
25. S. A. Adonin, I. D. Gorokh, A. S. Novikov, P. A. Abramov, M. N. Sokolov, V. P. Fedin, *Chem. Eur. J.*, 2017, **23**, 15612; DOI: 10.1002/chem.201703747.
26. S. A. Adonin, I. D. Gorokh, A. S. Novikov, P. A. Abramov, M. N. Sokolov, V. P. Fedin, *CrystEngComm*, 2018, **20**, 7766; DOI: 10.1039/c8ce01749b.

27. I. D. Gorokh, S. A. Adonin, A. S. Noviko, A. N. Usoltsev, P. E. Plyusnin, I. V. Korolkov, M. N. Sokolov, V. P. Fedin, *Polyhedron*, 2019, **166**, 137; DOI: 10.1016/j.poly.2019.03.041.
28. Bruker, *SAINT (Version 8.38A)*, Bruker AXS Inc., Madison, Wisconsin, USA, 2017.
29. O. V. Dolomanov, L. J. Bourhis, R. J. Gildea, J. A. K. Howard, H. Puschmann, *J. Appl. Crystallogr.*, 2009, **42**, 339; DOI: 10.1107/S0021889808042726.
30. G. Sheldrick, *Acta Crystallogr. C*, 2015, **71**, 3; DOI: 10.1107/S2053229614024218.
31. Bruker, *APEX3 Software Package*, Bruker AXS, Version 2015.5-2, 2015.
32. SADABS; *part of Bruker APEX3 Software Package*, Bruker AXS, version 2016/2, 2016.
33. P. Kubelka, F. Munk, *Z. Tech. Phys.* (*Leipzig*), 1931, **12**, 593.
34. S. A. Adonin, M. N. Sokolov, V. P. Fedin, *Coord. Chem. Rev.*, 2016, **312**, 1; DOI: 10.1016/j.ccr.2015.10.010.
35. T. Poręba, M. Ernst, D. Zimmer, P. Macchi, N. Casati, *Angew. Chem. Int. Ed.*, 2019, **58**, 6625; DOI: 10.1002/ange.201901178.
36. M. Węcławik, P. Szklarz, W. Medycki, R. Janicki, A. Piecha-Bisiorek, P. Zieliński, R. Jakubas. *Dalton Trans.*, 2015, **44**, 18447; DOI: 10.1039/C5DT02265G.
37. E. V. Savinkina, D. V. Golubev, M. S. Grigoriev, D. V. Albov, *Polyhedron*, 2013, **54**, 140; DOI: 10.1016/j.poly.2013.02.026.
38. P. H. Svensson, L. Kloo, *Chem. Rev.*, 2003, **103**, 1649; DOI: 10.1021/cr0204101.
39. Y.-Q. Hu, M.-Q. Li, Y. Wang, T. Zhang, P.-Q. Liao, Z. Zheng, X.-M. Chen, Y.-Z. Zheng, *Chem. Eur. J.*, 2017, **23**, 8409; DOI: 10.1002/chem.201702087.
40. A. Peuronen, H. Rinta, M. Lahtinen, *CrystEngComm*, 2015, **17**, 1736; DOI: 10.1039/C4CE01866D.
41. A. Hagfeldt, G. Boschloo, L. Sun, L. Kloo, H. Pettersson, *Chem. Rev.*, 2010, **110**, 6595; DOI: 10.1021/cr900356p.
42. A. J. Dennington, M. T. Weller, *Dalton Trans.*, 2016, **45**, 17974; DOI: 10.1039/C6DT03602C.
43. T. Li, Q. Wang, G. S. Nichol, C. A. Morrison, H. Han, Y. Hu, N. Robertson, *Dalton Trans.*, 2018, **47**, 7050; DOI: 10.1039/C8DT00864G.
44. J. Laane, P. W. Jagodzinski, *Inorg. Chem.*, 1980, **19**, 44; DOI: 10.1021/ic50203a010.
45. I. D. Gorokh, S. A. Adonin, A. S. Novikov, A. N. Usoltsev, P. E. Plyusnin, I. V. Korolkov, M. N. Sokolov, V. P. Fedin, *Polyhedron*, 2019, **166**, 137; DOI: 10.1016/j.poly.2019.03.041.
46. T. A. Shestimerova, N. A. Golubev, A. V. Mironov, M. A. Bykov, A. V. Shevelkov, *Russ. Chem. Bull.*, 2018, **67**, 1212; DOI: 10.1007/s11172-018-2204-6.
47. C. B. Aakeröy, T. A. Evans, K. R. Seddon, I. Pálinkó, *New J. Chem.*, 1999, **23,** 145-152; DOI: 10.1039/A809309A.
48. C. Hrizi, A. Trigui, Y. Abid, N. Chniba-Boudjada, P. Bordet, S. Chaabouni, *J. Solid State Chem.*, 2001, **184**, 3336; DOI: 10.1016/j.jssc.2011.10.004.
49. T. A. Shestimerova, M. A. Bykov, Z. Wei, E. V. Dikarev, A. V. Shevelkov, *Russ. Chem. Bull.*, 2019, **68**, 1520; DOI: 10.1007/s11172-019-2586-0.
50. T. A. Shestimerova, A. V. Shevelkov, *Russ. Chem. Rev.*, 2018, **87**, 28; DOI: 10.1070/RCR4762.
51. W. H. Oswald, E. M. Mozur, I. P. Moseley, H. Ahn, J. R. Neilson, *Inorg. Chem.*, 2019, **58**, 5818; DOI: 10.1021/acs.inorgchem.9b00170.

*Received May 31, 2020;*
*in revised form August 3, 2020;*
*accepted October 15, 2020*